Urban Climate 56 (2024) 102020

Contents lists available at ScienceDirect

Urban Climate

journal homepage: www.elsevier.com/locate/uclim

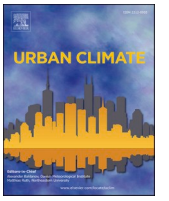

Environmental impacts of aerosol radiative effect and urbanization and their interactions over the Beijing-Tianjin-Hebei City cluster

Zilin Wang [a,b], Xin Huang [a,b,c,*], Qianqian Huang [d], Aijun Ding [a,b,c]

[a] School of Atmospheric Sciences, Nanjing University, Nanjing, China
[b] Jiangsu Provincial Collaborative Innovation Center for Climate Change, Nanjing, China
[c] Frontiers Science Center for Critical Earth Material Cycling, Nanjing University, Nanjing, China
[d] Institute of Urban Meteorology, China Meteorological Administration, Beijing, China

ARTICLE INFO

Keywords:
Urbanization
Air pollution
Aerosol radiative effect
Urban heat island
WRF-Chem

ABSTRACT

With fast economic development, urban expansion and air pollution are two main eco-environmental challenges confronting China. Though both are associated with intensified human activities, their impacts on urban environment are investigated separately, and the synthetic effect and intricate interaction of the two have not been fully understood. Here, based on in-situ measurements and online-coupled meteorology-chemistry modelling, the impacts of anthropogenic aerosol and urbanization are investigated simultaneously at Beijing-Tianjin-Hebei city cluster during a typical pollution season. The two processes exhibit opposite influences on meteorology and air quality. Aerosol via its radiative effect tends to cause net loss of solar energy with 3 °C cooling at the ground surface and 1 °C warming in the upper boundary layer. In contrast, urbanization yields large increment of net surface solar radiation as well as sensible heat flux, leading to over 1 °C warming in the lower atmosphere. Such modifications of boundary layer structure alter the accumulation and formation of air pollution. Urbanization effect dominated in the modification of near-surface air temperature and air pollution, making the synthetic effect a linear combination of two processes. The study highlights a comprehensive understanding of air pollution and urbanization and their synergy effect on urban environment over megacities.

1. Introduction

The fast development of economy and society brings great challenges to the earth climate system. As one crucial anthropogenic impact, rapid urban expansion leads to dramatic changes in the underlying surface properties (Kalnay and Cai, 2003). Specifically, impervious urban surface with lower albedo could increase the absorption of solar radiation and inhibit evapo-transpiration, and hence perturb surface energy budget and meteorology especially precipitation in the city and downwind areas (Lo et al., 2007; Tao et al., 2015; X. Yang et al., 2011). Evidence suggests that convective activities and the movement of storms may also be disturbed by urban surfaces (Zhong et al., 2015). Combined with anthropogenic heat released from fuel combustion and air conditioning, urban areas exhibit a distinct temperature increment in comparison with rural areas, which is well acknowledged as urban heat island (UHI) effect (Oke, 1973, 1982). Therefore, the structure of urban boundary layer differs remarkably from rural counterparts, associated with

* Corresponding author at: School of Atmospheric Sciences, Nanjing University, Nanjing, China
E-mail address: xinhuang@nju.edu.cn (X. Huang).

https://doi.org/10.1016/j.uclim.2024.102020
Received 1 February 2024; Received in revised form 17 April 2024; Accepted 14 June 2024
Available online 24 June 2024

heat stress and health risks (Frehlich et al., 2006; Li et al., 2016; S. Miao et al., 2009; Sarrat et al., 2006).

Intensive human activities in urban areas produce not only land use change and anthropogenic heat but also tons of atmospheric pollutant emissions, leading to severe air pollution. High loadings of $PM_{2.5}$ could exert negative impacts on both human health as well as regional climate and environment (Buseck and Pósfai, 1999; Charlson et al., 1992). Plenty of suspended aerosols in urban areas perturb radiation budget of the earth system by directly interacting with the solar/terrestrial radiation and indirectly participating in cloud microphysics (Albrecht, 1989; Ramanathan et al., 2001). Global average climate forcing caused by radiative effect of aerosols is estimated to be -1 W m^{-2}, with great temporal and spatial variations (X. Huang et al., 2015; Kim, 2005; Masson-Delmotte et al., 2021). Studies have reported that aerosol can also alter multi-scale atmospheric circulations such as Asian monsoon and regional convective precipitation (Fan et al., 2015; Meehl et al., 2008). Moreover, radiatively active aerosols can play an important role in altering planetary boundary layer (PBL) stability, triggering a positive feedback between aerosol and PBL meteorology called aerosol-PBL interaction (Ding et al., 2016; J. Wang et al., 2014; H. Yu et al., 2002).

As the largest developing country, China's economic boom has been accompanied by rapid urbanization. The Beijing-Tianjin-Hebei (BTH) city cluster on the north of North China Plain consists of Beijing municipality, Tianjin municipality and Hebei Province, covering an area of 216,000 km^2 with population exceeding 100 million. Pronounced UHI effect has been identified over the BTH city cluster using meteorological station observations or land surface temperature retrieved from satellite products (Ren et al., 2007; P. Yang et al., 2013), which contributed to the warming trends over the past 50 years (L. Zhou et al., 2004). Considering its unique geographic location, the influence of sea-land breeze and mountain-valley breeze further complicates the local circulations over urban areas (Y. Miao et al., 2015). In addition, due to growing emissions of gases and aerosol precursors from industry, energy production and traffic, BTH city cluster became a noticeable hotspot for air pollution. Under stagnant synoptic conditions, high loadings of aerosol make the region one of the most heavily polluted areas in the world (Jiang et al., 2015; Sun et al., 2014; Zheng et al., 2015). Therefore, the impacts of both urbanization and aerosol on regional climate and environment are remarkable in the BTH city cluster.

Although studies have explored impacts of urbanization and aerosol pollution separately, the synthetic effect and intricate interaction have not been fully understood. Based on multiple observations and online-coupled meteorology-chemistry simulations, the impacts of aerosol radiative effect and urbanization on urban meteorology and air quality over BTH city cluster during a typical heavily-polluted season were investigated and compared in details. The synthetic effect and possible interaction between these two processes are illustrated as well. The remainder of this paper is organized as follows. Section 2 decribes the observational data and numerical experiments with detailed model configuration. Results and discussions are presented in Section 3, followed by conclusions summarized in section 4.

2. Data and methods

2.1. Observational data

In this study, land use type is identified by MODerate resolution Imaging Spectroradiometer (MODIS) land cover product (MCD12Q1) with IGBP classification, which is derived using supervised classifications of MODIS reflectance data at a resolution of 500 m. Satellite-retrieved aerosol optical depth (AOD) at 550 nm provided by MODIS Collection 6.1 with a horizontal resolution of 10 km $\times$ 10 km was applied to depict spatial distribution of aerosol pollution. MODIS data products of land cover and aerosol properties can all be ordered at https://ladsweb.modaps.eosdis.nasa.gov/search/.

Hourly meteorological fields including air temperature, relative humidity as well as surface winds archived at US National Climate Data Center were collected to represent real-time meteorological conditions (https://www.ncei.noaa.gov/data/global-hourly/access). $PM_{2.5}$ concentrations released by Ministry of Ecology and Environment of China have been analyzed to reveal spatiotemporal variations of surface aerosol pollution (https://www.cnemc.cn). Atmospheric vertical profiles at Beijing (39.93 ^{o}N, 116.28°E) were detected twice a day at 00 and 12 UTC by radiosondes (http://weather.uwyo.edu/upperair/sounding.html). Air temperature, wind and water mixing ratio were reported on primarily mandatory pressure levels for the lower troposphere.

Observation minus forecast (OMF) analysis is adopted here to show the influence of aerosol and urbanization on the boundary layer struture. 24-h forecast results from Global Forecast System (GFS, https://rda.ucar.edu/datasets/ds084.6/) were compared with real-time observations from in-situ monitoring stations. The GFS model with a spatial resolution of $0.25^{o} \times 0.25^{o}$ is run without considering the effect of land-use change or aerosol. Hence, disparities between atmospheric sounding/surface observations and the forecast datasets could somehow reflect the perturbations induced by these factors. Such methods have been successfully applied to reveal the impact of urbanization and land-use change on climate (Kalnay and Cai, 2003) as well as the aerosol's influence on meteorology (X. Huang and Ding, 2021).

2.2. Numerical experiments

Multiple numerical experiments were conducted using regional online-coupled meteorology-chemistry model WRF-Chem version 3.7 (Grell et al., 2005). We adopted two nested model domains (Fig. S1). The spatial resolution of the parent domain is 20 km which covers eastern China and its surrounding areas, while the inner domain applies a 4 km grid interval over BTH city cluster. The vertical grid contains 40 sigma levels from the surface to 50 hPa. Half of the total layers are placed below 1 km to better describe boundary layer processes with the first layer being approximately 10 m. The simulation is conducted for the whole month of December 2016. Each run lasts for 36 h and the last 24-h results were analyzed. The first 5-day integration is considered as model spin-up to acquire regional atmospheric chemistry background, and the chemical outputs from the previous run are used as the initial conditions for the

following run. The initial and lateral boundary conditions of meteorological fields are provided by National Center for Environmental Prediction Final Analysis data with $1^o \times 1^o$ spatial resolution and 6-h interval.

Key physical parameterization options for the WRF-Chem modelling are Lin microphysics scheme with the Grell cumulus parameterization to reproduce the cloud and precipitation processes (Grell and Dévényi, 2002; Lin et al., 1983). The sophisticated Noah land surface scheme developed by Ek et al. (2003) is used to describe the land-atmosphere interactions, including detailed land surface processes of thermodynamics and hydrology, such as moisture diffusion and evapo-transpiration. Rapid Radiative Transfer Model shortwave and longwave radiation scheme (Iacono et al., 2008) combined with Yonsei University PBL scheme (Hong et al., 2006) is applied to describe aerosol radiative effect and its influence on PBL meteorology. For the numerical representation of atmospheric chemistry, we used the Carbon-Bond Mechanism version (Zaveri and Peters, 1999) photochemical mechanism along with Model for Simulating Aerosol Interactions and Chemistry aerosol model (Zaveri et al., 2008). Aerosols of 11 species are separated into four bins (0.039–0.156, 0.156–0.625, 0.625–2.5, and 2.5–10 μm) according to their dry diameter. The assumptions of spherical particles and internally mixing are made in each bin to compute optical properties of aerosol based on Mie theory. Physical and chemical schemes applied are summarized in Table S1.

Monthly anthropogenic emissions of aerosols and its precursors were obtained from Multi-resolution Emission Inventory for China (MEIC) (Li et al., 2017b). Emissions of major pollutants, such as CO, SO_2, NO_x, NH_3 and speciated VOCs from five sectors including power plants, residential combustion, industry, transportation and agricultural activities for the year 2016 are all included. Further, MEGAN (Model of Emissions of Gases and Aerosols from Nature) module embedded in WRF-Chem model is used to calculate biogenic emissions online. Soil-derived dust emissions and sea salt emissions are described by GOCART emission scheme.

A single-layer urban canopy model (UCM) developed by Kusaka and Kimura (2004) is coupled into WRF-Chem to simulate urban meteorology. The UCM model recognizes the three-dimensional nature of the urban surface, considering the shadowing, reflections and the trapping of radiation in a street canyon. Treated as a part of the sensible heat flux, anthropogenic heat (AH) is included in the study characterized by a diurnal cycle with two peaks at rush hours of 08 and 17 Local Time. The peak value of AH is assigned to be 90 W m^{-2} (Allen et al., 2010; Tewari et al., 2007; M. Yu et al., 2014). The total sensible heat flux from roof, wall, roads and the urban canyon is then passed to land surface model. For a given WRF grid cell, the Noah land surface model calculates surface fluxes and temperature for vegetated areas (such as trees and parks) and the UCM provides the fluxes for urban surfaces (F. Chen et al., 2011).

Four experiments are conducted with identical domain setting and parameterizations except for different consideration of aerosol radiative effect and urbanization effect (Table S2). In order to represent urbanization effect, land cover in the model are updated using MCD12Q1 of the year 2016 and then proceed with UCM (EXP_ARI0_URB1). Urban grid points in the control experiment are all subscribed with surrounding vegetation categories (L. Chen et al., 2018; S. Miao et al., 2009; N. Zhang et al., 2010), mainly croplands (EXP_ARI0_URB0). The disparities between EXP_ARI0_URB1 and EXP_ARI0_URB0 are attributed to the influence of urbanization. For aerosol direct radiative effect, the inclusion and exclusion of aerosol scattering and absorption in the radiation transfer are indicated by ARI0 and ARI1. The difference between EXP_ARI1_URB0 and EXP_ARI0_URB0 are attributed to aerosol-radiation interaction. Since aerosol-radiation interaction overwhelmed aerosol-cloud interaction in polluted urban areas (Rosenfeld, 2008), the aerosol indirect effect was excluded without further discussion in this study. The synthetic effect of these two processes is considered in EXP_ARI1_URB1.

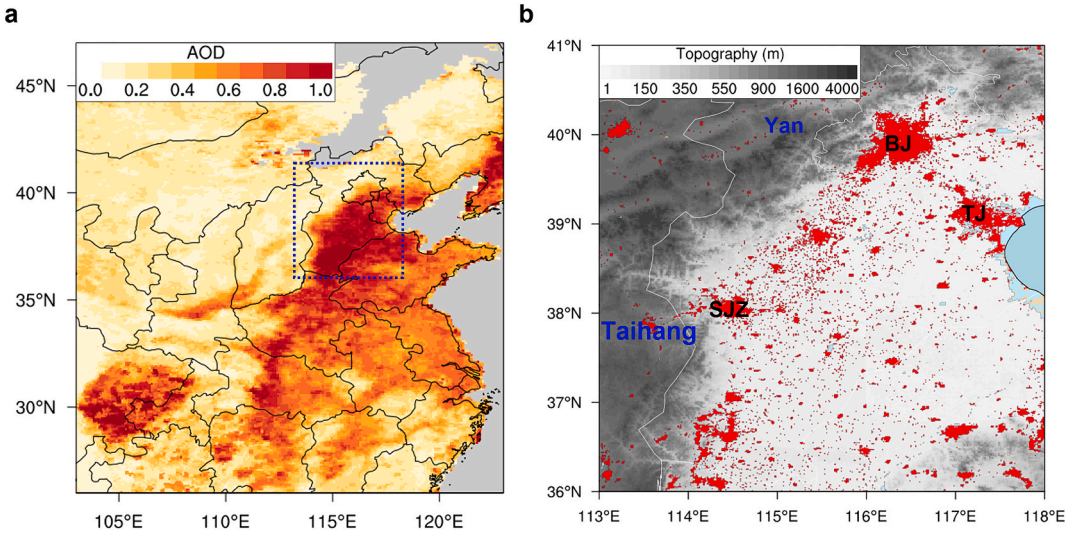

Fig. 1. (a) Average aerosol optical depth (AOD) derived from MODIS satellite retrievals during the winter of 2016 over eastern China. The blue rectangle encircled the Beijing-Tianjin-Hebei city cluster. (b) MODIS derived urban land cover (in red) of BTH region over its topography. Three main cities including Beijing (BJ), Tianjin (TJ), Shijiazhuang (SJZ) with Taihang Mountain and Yan Mountain are marked as well. (For interpretation of the references to colour in this figure legend, the reader is referred to the web version of this article.)

3. Results and discussions

3.1. Observational evidence of aerosol radiative effect and urbanization

The BTH city cluster is characterized with rapid urbanization and severe air pollution (Fig. 1). Although clean air actions have been implemented for years, heavy aerosol pollution still frequently strikes the region due to unfavorable meteorological conditions and half-open basin topography (X. Huang et al., 2020; X. G. Liu et al., 2013; Zheng et al., 2015). The maximum AOD during the winter of 2016 over BTH region exceeded 2.0, indicating a severe aerosol pollution. The most polluted area lies in the east of Taihang Mountain and south of Yan Mountain including three main cities: Beijing, Tianjin and Shijiazhuang. Wintertime air quality of this region varies with mid-latitude synoptic systems especially cold fronts. Such variations were illustrated by daily $PM_{2.5}$ shown in Fig. 2a. Beijing experienced five pollution episodes from the beginning of December 2016 to the end of January 2017, with an average daily $PM_{2.5}$ concentration exceeding 75 μg m^{-3} (Fig. 2a).

Distinct differences were identified when comparing the atmospheric temperature profile detected by radiosonde with GFS forecasts, namely OMF analysis, under clean and polluted conditions at Beijing (Figs. 2b-2c). Here, clean and polluted days were classified based on their daily $PM_{2.5}$ concentration, which are denoted by blue and red dots in Fig. 2a. Specifically, daily $PM_{2.5}$ greater than (less than) 75th percentile (25th percentile) is defined as a polluted (clean) day, and days with clouds or precipitation were excluded. As shown, the OMF results exhibited a stabilized stratification under polluted conditions, i.e., upper-level warming and near-surface cooling, which can be mainly attributed to radiative effect of aerosols. Scattering and absorption of aerosols reduced the incident solar radiation, decreased surface sensible heat flux and hence near-surface temperature, which accounted for the cold bias as large as 3 °C at 1000 hPa. In addition, absorbing aerosols trapped part of the incident solar energy in the lower atmosphere, increased the shortwave heating rate and subsequently led to atmospheric warming approximate to 1 °C. Such inversions are frequently observed during the winter and are related to aerosol pollution over eastern China (Q. Huang et al., 2021; X. Huang et al., 2018).

In contrast, the OMF analysis for clean days showed a positive bias >1 °C at the surface and decrease monotonically along the altitude to about 800 hPa (Fig. 2b). In other words, the observed air temperature in the lower atmosphere is usually warmer than expected by the forecast model without considering the anthropogenic influences. A highly possible explanation is the more pronounced urban heat island effect on clean days. Lower surface albedos, higher Bowen ratio and the increase of surface energy storage in urban areas tend to perturb the surface energy budget, resulting in higher near-surface temperature in cities (Chakraborty et al., 2016;

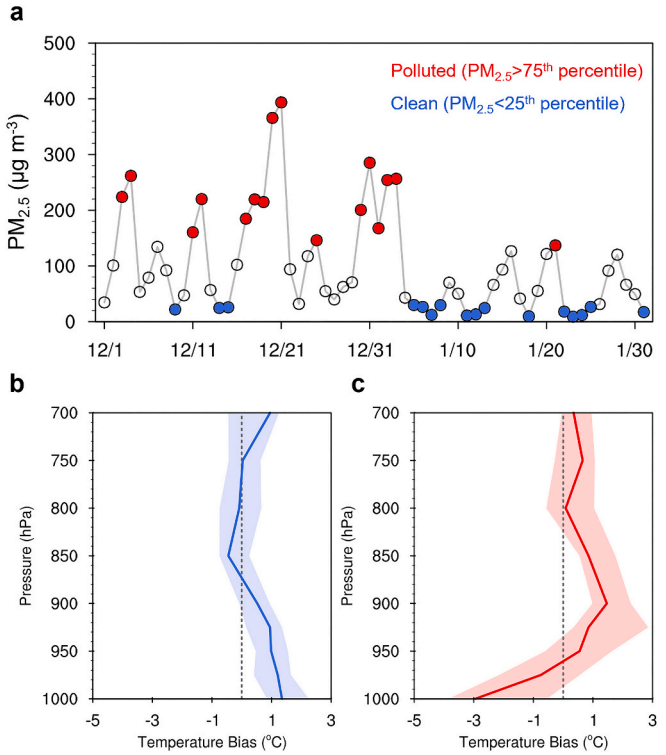

Fig. 2. (a) Variations of daily average surface $PM_{2.5}$ concentration in Beijing during the winter of 2016–2017. $PM_{2.5}$ concentrations lower than 25th percentile (larger than 75th percentile) are marked in blue (red) to represent the clean (polluted) days. (b) Vertical profiles of OMF analysis under clean conditions at Beijing. Solid lines and shaded areas indicate the average and 25-75th percentile. Zero line in grey dashed pattern is shown for reference. (c) Same as (b) but for polluted conditions. (For interpretation of the references to colour in this figure legend, the reader is referred to the web version of this article.)

D. Zhou et al., 2016). Such a warming at lower urban boundary layer is further confirmed by numerical simulations under the influence of urbanization.

3.2. The respective impacts of aerosol and urbanization on urban environment

To quantitatively understand impacts of aerosol and urbanization, model simulations were conducted using WRF-Chem, and then evaluated against observations to verify model's ability to reproduce the actual meteorology and chemistry fields. Generally, the simulated meteorological variables agree well with the measurements (Fig. S2). The mean bias of air temperature and relative humidity (RH) at ground surface are −0.83 °C and − 10%, with correlation coefficients approximate to 0.8 and 0.6, respectively. The model slightly overestimated the observed wind speed, resulting in a positive mean bias of 0.6 m s^{-1}, which could be attributed to the coarse topography used in the study. Vertical profile of atmospheric temperature is also captured reasonably well compared with radiosonde observations, indicating that the model can describe the atmospheric stratification as well as PBL processes (Fig. S3). As for spatial and temporal variations of air pollutants, time series and spatial distribution of $PM_{2.5}$ from simulations and real-time measurements are shown in Figs. S4-S5. The magnitudes and variations of $PM_{2.5}$ could be reproduced generally well with some overestimations during the polluted episodes, probably due to uncertainties in emission inventory and sub-grid scale parameterizations.

According to WRF-Chem simulations, surface energy budget was greatly modified by urbanization and aerosol radiative effect (Fig. 3). Owing to lower surface albedo at urban areas, the net solar radiation at surface increased by about 20 W m^{-2} under the influence of urbanization. Correspondingly, sensible heat flux at surface increased, with a magnitude larger than the increment of net surface shortwave radiation, probably due to the release of anthropogenic heat. Such energy modifications caused by urbanization centered at urban region with limited influence on surrounding areas. In contrast to urbanization, aerosol radiative effect exerts perturbation over a relatively large scale and exhibited prominent regional disparities. The decrease of the net surface solar radiation

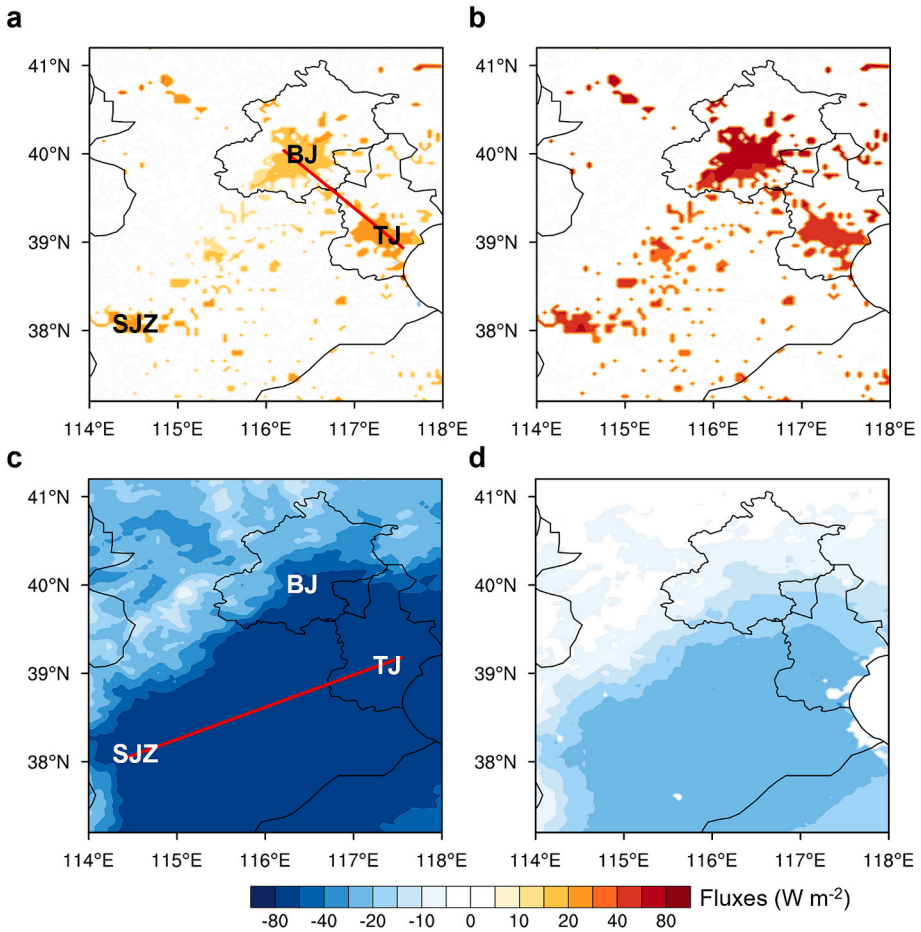

Fig. 3. Average perturbations of (a) net surface solar radiation and (b) sensible heat flux at surface due to urbanization during the winter of 2016. The same for (c) and (d) but caused by aerosol radiative effect. The red lines in (a) and (c) represent the vertical cross-sections to reveal the influences of urbanization and aerosol radiative effect on boundary layer in Figs. 4–5. Main cities including Beijing (BJ), Tianjin (TJ) and Shijiazhuang (SJZ) are marked on the map. (For interpretation of the references to colour in this figure legend, the reader is referred to the web version of this article.)

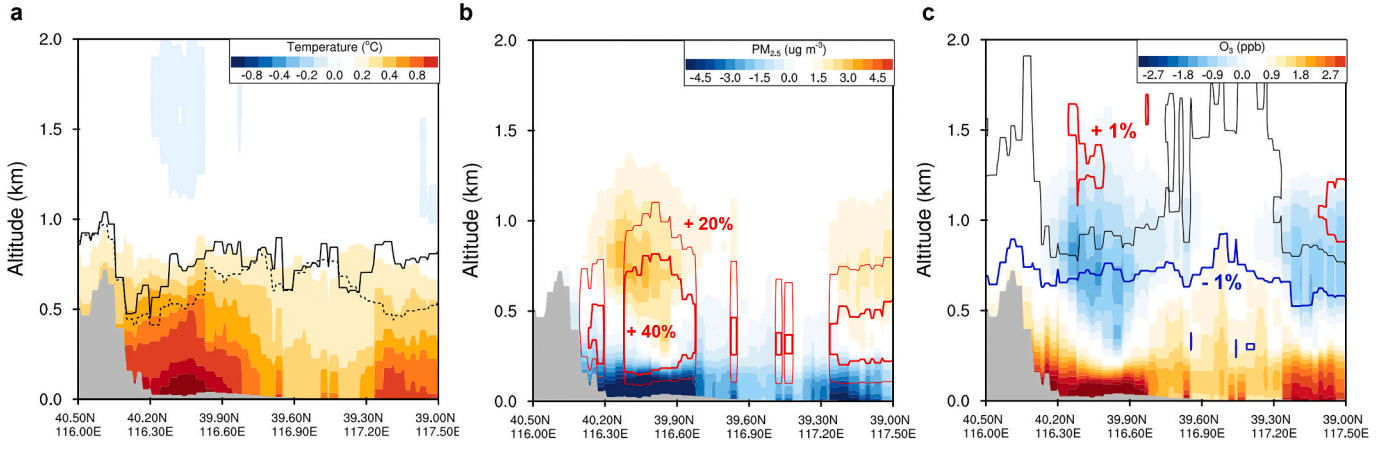

Fig. 4. Cross-section of average perturbations induced by urbanization within boundary layer along BJ-TJ axes during the winter of 2016. (a) Air temperature (shading) and boundary layer height (solid line for EXP_ARI0_URB1 and dashed line for EXP_ARI0_URB0). (b) $PM_{2.5}$ concentration (shading) and turbulent exchange coefficient (contour line labelled with changing percent). (c) O_3 concentration (shading) and relative humidity (contour line labelled with changing magnitude).

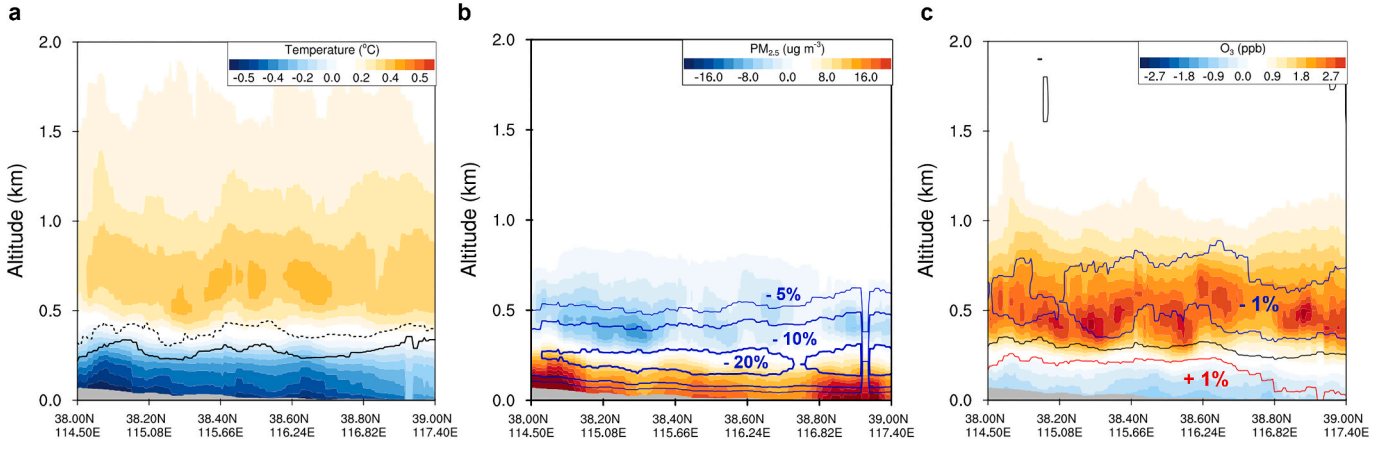

Fig. 5. Cross-section of average perturbations induced by aerosol radiative effect within boundary layer along BJ-TJ axes during the winter of 2016. The variables presented are the same as Fig. 4.

resembled the distribution of AOD which showed a positive gradient from south to north. With the averaged AOD being 0.56 and surface $PM_{2.5}$ concentration being 150 μg m^{-3}, the maximum reduction of the solar radiation at surface reached as high as 80 W m^{-2}. Accordingly, the sensible heat flux also decreased by 30%, indicating a decline of buoyancy from the ground surface for PBL development.

Modifications in meteorology and chemistry within the boundary layer induced by these two processes are analyzed as well (Fig. 4). As has been previously revealed by OMF results in Fig. 2b, urbanization may result in near-surface warming, also known as UHI effect. The warming due to urbanization reached 1.1, 0.5 and 0.3 °C at Beijing, Tianjin and Shijiazhuang, and decreased linearly along the altitude to about 500 m. The different warming magnitudes are associated with city size and population (Manoli et al., 2019; Memon et al., 2008). A reduction in RH as well as water vapor mixing ratio was expectable given the concrete surface and less vegetation in the urban areas. The near-surface warming promoted the turbulent mixing and the daytime development of PBL, which was further confirmed by the pronounced increase of PBL height and turbulent exchange coefficient. Moreover, the near-surface warming forced a low-pressure anomaly and hence created convergent air flow over the urban areas. Such a convergence along with the updrafts over urban region made up the UHI circulation, which favored the vertical transport within PBL as well as the dispersion of air pollutants. Correspondingly, $PM_{2.5}$ reduction and increment was identified near the surface and at upper-level above, up to 20 and 3 μg m^{-3}, respectively. However, as another important atmospheric pollutant, surface O_3 was found to increase, probably due to higher temperature and more vigorous photochemistry (P. Liu et al., 2020; Otero et al., 2016). It should be noted that the upward transport of urban air pollution by UHI circulation may affect air quality in downwind suburban or rural areas, and even worsen the urban air quality once again through the surface convergence.

On the contrary, the influence of aerosol radiative effect is almost opposite to urbanization (Fig. 5). Near-surface air temperature could drop nearly 1 °C since the incident solar energy are blocked by aerosols. Simultaneously, atmospheric warming induced by absorbing aerosols reached about 0.5 °C, greatly contributing to the stable stratification within the boundary layer. The vertical temperature profile altered by scattering and absorbing aerosols was in accordance with the OMF analysis under polluted conditions in Fig. 2c. Therefore, insufficient surface buoyancy combined with stabilized lower troposphere greatly suppressed the vertical mixing of the air mass and the development of PBL, which is indicated by over 20% reduction of turbulent exchange coefficient in Fig. 5b. Such modifications also facilitated the subsequent accumulation of air pollutants emitted from the urban surface. Compared with the simulation excluding aerosol's effect, the average reduction of the PBL height and the enhancement of $PM_{2.5}$ concentration are estimated to be 120 m and 15 μg m^{-3}, respectively. Due to slower reaction rates in a dimming and cooler atmosphere, surface O_3 decreased by about 1 ppb (Otero et al., 2016). The two-way interaction between aerosol and the PBL meteorology has been reported in regional air pollution in eastern China (Ding et al., 2016; Li et al., 2017a; Z. Wang et al., 2018) and plays an important role in the aggravation of aerosol pollution (Dong et al., 2017; Slater et al., 2020; Su et al., 2022; X. Zhang et al., 2018). Considering the opposite impacts of aerosol and urbanization over urban areas, it is essential to explore their synthetic influence.

3.3. *The synergy effect of aerosol and urbanization with their interactions*

The influences of aerosol and urbanization are coupled with each other and may vary with different air pollution levels, resulting in synthetic impact and intricate interaction of two processes. Here, perturbations of near-surface air temperature and $PM_{2.5}$ concentration are adopted to illustrate the magnitude of aerosol radiative effect and urbanization, and their response to changing aerosol

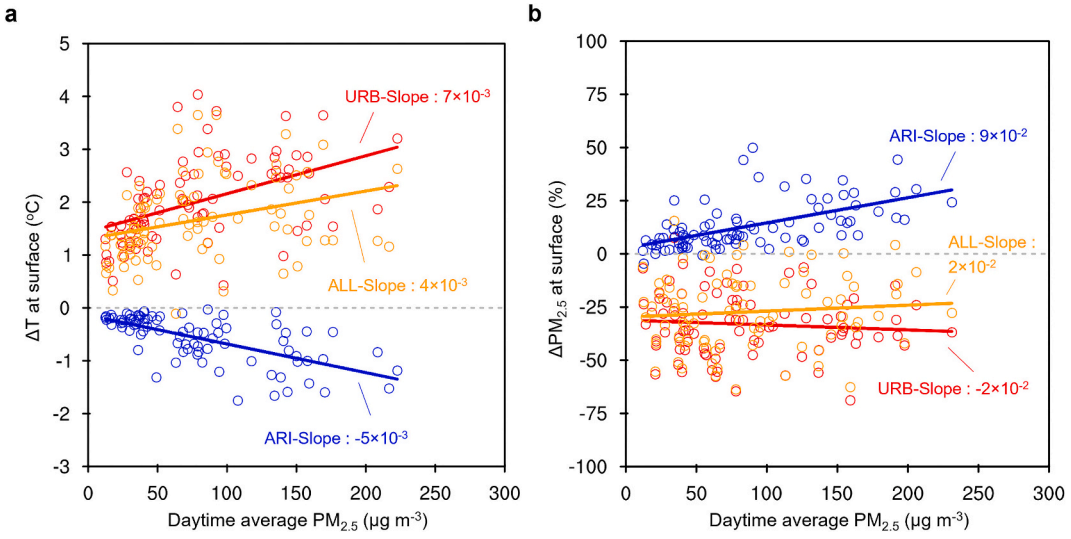

Fig. 6. Separate and synthetic effects of aerosol and urbanization vary with different air pollution levels at three main cities in BTH city cluster. (a) Perturbations of near-surface air temperature caused by aerosol radiative effect and urbanization along with daytime average $PM_{2.5}$ concentration. Regression lines are given with their slopes. (b) same as (a) but for perturbations of surface $PM_{2.5}$ concentration.

pollution level was shown in Fig. 6. The perturbations in air temperature and $PM_{2.5}$ concentration due to urbanization are always larger than aerosol radiative effect, suggesting the dominant effect of urbanization at all pollution levels. Moreover, the perturbations in response to various aerosol pollution level was demonstrated. According to the impact of aerosol radiative effect illustrated bofore, it is predictable that the reduction of near-surface air temperature and the enhancement of surface $PM_{2.5}$ would increase with elevated aerosol loadings, exhibiting a changing slope of -5×10^{-3} °C/(μg m^{-3}) and 9×10^{-2}%/(μg m^{-3}), respectively. In contrast, the air temperature perturbations caused by urbanization increased with higher aerosol loading, with the slope of the fitting line being 7×10^{-3} °C/(μg m^{-3}), indicating that the urbanization effect was also sensitive to aerosol pollution level. In all, urbanization effect dominates in the modification of near-surface air temperature and air quality, making the synthetic effect a linear combination of two processes. Also, it can be inferred that with increasing aerosol pollution level, urbanization effect consistently prevails over aerosol radiative effect. Notebly, the maximum value of AH applied in the model may be overestimated since all urban grids are assumed to be highly-commercial region with the highest AH emission (Tewari et al., 2007). Therefore, the relative importance of urbanization may be overvalued with uncertainties.

Surprisingly, the near-surface warming caused by urbanization showed a positive correlation with $PM_{2.5}$ concentration, indicating that aerosol may act to enhance UHI intensity (Fig. 7a). The average UHI intensity (indicated by air temperature perturbations induced by urbanization) is 1 °C when daytime average $PM_{2.5}$ is 50 μg m^{-3} and increased to almost 3 °C when $PM_{2.5}$ reaches 200 μg m^{-3}. Such a relationship was also reported in several cities with observational and experimental methods (Han et al., 2020; Jonsson et al., 2004; G. Yang et al., 2021), especially during polluted days in Beijing (L. Chen et al., 2018). Two atmospheric processes may take responsibility for the intensification of urban warming with higher $PM_{2.5}$ concentration. Compared with simulation excluding aerosol radiative effect, the urban boundary layer are more stable with smaller turbulent exchange coefficient under the influence of aerosol (Fig. 7b). The weakened turbulence not only confines more pollutants to a shallower PBL, but also prevents the transport and diffusion of heat released, which contributes to the reinforcement of UHI intensity (Han et al., 2020). Additionally, apart from the attenuation of shortwave radiation, aerosol may also interfere with longwave radiation, reflected by an increase in downwelling longwave radiation at surface and a reduction of outgoing longwave radiation (OLR) of the earth system. Such an influence of aerosol acts much like a thin low cloud warming the atmosphere, which aggravates the warming in urban areas (Cao et al., 2016). Considering the interaction of urbanization and aerosol radiative effect, lower $PM_{2.5}$ concentration under more restrict emission policy may contribute to the mitigation of UHI during the winter in the future.

4. Conclusions

Fast urban expansion and intensive emissions of air pollutants are two of the most important aspects of human activities, yet their impacts on urban environment are often investigated separately. Based on in-situ measurements and online-coupled meteorology-chemistry numerical simulations, the synthetic impact and intricate interaction of aerosol radiative effect and urbanization are investigated simultaneously at BTH city cluster. Respective impacts of urbanization and anthropogenic aerosol on urban meteorology and air quality are revealed and compared in details. Aerosol radiative effect tends to produce net loss of solar energy at the surface, which dominates the polluted days with 3 °C cooling at ground surface and 1 °C warming in the upper boundary layer. Such modifications of boundary layer structure favor the accumulation of air pollution, indicated by 10% increase of surface $PM_{2.5}$ in average. In contrast, urbanization yields large increment of net surface solar radiation and sensible heat flux, which is more prominent during clean days, leading to over 1 °C warming in the lower atmosphere. The buoyancy supported by surface warming and UHI circulation

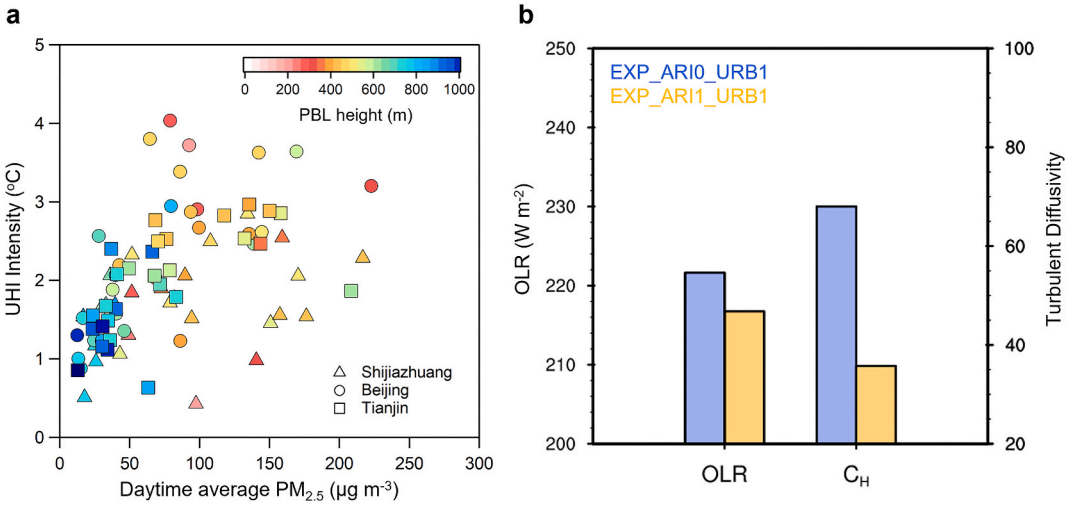

Fig. 7. (a) Relationships of daytime average $PM_{2.5}$ concentration and UHI intensity for three main cities in BTH city cluster. Markers are colored with daytime PBL height. (b) Comparison of daytime average outgoing longwave radiation (OLR) and turbulent exchange coefficient between simulation scenario EXP_ARI1_URB1 and EXP_ARI0_URB1.

over urban surface is conducive to the vertical transport and dispersion of air pollution. In all, the two processes exhibit opposite influences on meteorology and air quality.

Furthermore, the synthetic effect and intricate interaction of urbanization and aerosol are illustrated both in simulations and observations. The near-surface warming caused by urbanization showed a positive correlation with $PM_{2.5}$ concentration, indicating that aerosol may act to enhance UHI effect via increasing the stability of boundary layer and perturbing longwave radiation budget. Urbanization effect dominated in the modification of near-surface air temperature and aerosol pollutant, making the synthetic effect a linear combination of two processes. With more restricted emission control strategy such as carbon peak and carbon neutrality goals implemented in the future, negative impacts of aerosol on human health and urban environment could be greatly reduced in China, and may contribute to the mitigation of UHI during the winter. However, the on-going development of city clusters into megacities or gigacities may further amplify urbanization effect and complicate its circulation pattern. The study promotes a comprehensive understanding of air pollution and urbanization as well as their interactions over megacities.

Funding resources

This work was supported by the National Natural Science Foundation of China (42305117, 42293322), the Key Laboratory of Urban Meteorology (LUM-2023-09) and Fundamental Research Funds for the Central Universities (14380198).

CRediT authorship contribution statement

Zilin Wang: Writing – original draft, Validation, Methodology, Investigation. **Xin Huang:** Writing – review & editing, Supervision. **Qianqian Huang:** Visualization, Resources, Data curation. **Aijun Ding:** Supervision, Conceptualization.

Declaration of competing interest

The authors declare that they have no known competing financial interests or personal relationships that could have appeared to influence the work reported in this paper.

Data availability

Data will be made available on request.

Acknowledgments

We are grateful to the high-performance computing center of collaborative innovation center of advanced microstructures of Nanjing University for conducting analysis and calculations in this paper.

Appendix A. Supplementary data

Supplementary data to this article can be found online at https://doi.org/10.1016/j.uclim.2024.102020.

References

Albrecht, B.A., 1989. Aerosols, cloud microphysics, and fractional cloudiness. Science 245 (4923), 1227–1230. Retrieved from. http://www.jstor.org/stable/1704234.

Allen, L., Lindberg, F., Grimmond, C.S.B., 2010. Global to city scale urban anthropogenic heat flux: model and variability. Int. J. Climatol. 31 (13), 1990–2005. https://doi.org/10.1002/joc.2210.

Buseck, P., Pósfai, M., 1999. Airborne minerals and related aerosol particles: effects on climate and the environment. Proc. Natl. Acad. Sci. USA 96, 3372–3379. https://doi.org/10.1073/pnas.96.7.3372.

Cao, C., Lee, X., Liu, S., Schultz, N., Xiao, W., Zhang, M., Zhao, L., 2016. Urban heat islands in China enhanced by haze pollution. Nat. Commun. 7, 12509 https://doi.org/10.1038/ncomms12509.

Chakraborty, T., Sarangi, C., Tripathi, S.N., 2016. Understanding Diurnality and inter-seasonality of a sub-tropical urban Heat Island. Bound.-Layer Meteorol. 163 (2), 287–309. https://doi.org/10.1007/s10546-016-0223-0.

Charlson, R., Schwartz, S., Hales, J., Cess, R., Coakley, Jr, Hansen, J., Hofmann, D., 1992. Climate forcing by anthropogenic aerosols. Science 255, 423–430. https://doi.org/10.1126/science.255.5043.423.

Chen, F., Kusaka, H., Bornstein, R., Ching, J., Grimmond, C.S.B., Grossman-Clarke, S., Zhang, C., 2011. The integrated WRF/urban modelling system: development, evaluation, and applications to urban environmental problems. Int. J. Climatol. 31 (2), 273–288. https://doi.org/10.1002/joc.2158.

Chen, L., Zhang, M., Zhu, J., Wang, Y., Skorokhod, A., 2018. Modeling impacts of urbanization and urban Heat Island mitigation on boundary layer meteorology and air quality in Beijing under different weather conditions. J. Geophys. Res. Atmos. 123 (8), 4323–4344. https://doi.org/10.1002/2017jd027501.

Ding, A., Huang, X., Nie, W., Sun, J., Kerminen, V.M., Petäjä, T., Fu, C.B., 2016. Enhanced haze pollution by black carbon in megacities in China. Geophys. Res. Lett. 43 (6), 2873–2879. https://doi.org/10.1002/2016gl067745.

Dong, Z., Li, Z., Yu, X., Cribb, M., Li, X., Dai, J., 2017. Opposite long-term trends in aerosols between low and high altitudes: a testimony to the aerosol–PBL feedback. Atmos. Chem. Phys. 17 (12), 7997–8009. https://doi.org/10.5194/acp-17-7997-2017.

Ek, M.B., Mitchell, K.E., Lin, Y., Rogers, E., Grunmann, P., Koren, V., Tarpley, J.D., 2003. Implementation of Noah land surface model advances in the National Centers for environmental prediction operational mesoscale Eta model. J. Geophys. Res. Atmos. 108 (D22) https://doi.org/10.1029/2002jd003296.
Fan, J., Rosenfeld, D., Yang, Y., Zhao, C., Leung, L.R., Li, Z., 2015. Substantial contribution of anthropogenic air pollution to catastrophic floods in Southwest China. Geophys. Res. Lett. 42 (14), 6066–6075. https://doi.org/10.1002/2015gl064479.
Frehlich, R., Meillier, Y., Jensen, M.L., Balsley, B., Sharman, R., 2006. Measurements of boundary layer profiles in an urban environment. J. Appl. Meteorol. Climatol. 45 (6), 821–837. https://doi.org/10.1175/jam2368.1.
Grell, G.A., Dévényi, D., 2002. A generalized approach to parameterizing convection combining ensemble and data assimilation techniques. Geophys. Res. Lett. 29 (14) https://doi.org/10.1029/2002gl015311, 38-31-38-34.
Grell, G.A., Peckham, S.E., Schmitz, R., McKeen, S.A., Frost, G., Skamarock, W.C., Eder, B., 2005. Fully coupled "online" chemistry within the WRF model. Atmos. Environ. 39 (37), 6957–6975. https://doi.org/10.1016/j.atmosenv.2005.04.027.
Han, W., Li, Z., Wu, F., Zhang, Y., Guo, J., Su, T., Lee, S.-S., 2020. The mechanisms and seasonal differences of the impact of aerosols on daytime surface urban heat island effect. Atmos. Chem. Phys. 20 (11), 6479–6493. https://doi.org/10.5194/acp-20-6479-2020.
Hong, S.-Y., Noh, Y., Dudhia, J., 2006. A new vertical diffusion package with an explicit treatment of entrainment processes. Mon. Weather Rev. 134 (9), 2318–2341. https://doi.org/10.1175/mwr3199.1.
Huang, X., Ding, A., 2021. Aerosol as a critical factor causing forecast biases of air temperature in global numerical weather prediction models. Sci. Bull. 66 (18), 1917–1924. https://doi.org/10.1016/j.scib.2021.05.009.
Huang, X., Song, Y., Zhao, C., Cai, X., Zhang, H., Zhu, T., 2015. Direct radiative effect by multicomponent aerosol over China. J. Clim. 28 (9), 3472–3495. https://doi.org/10.1175/jcli-d-14-00365.1.
Huang, X., Wang, Z., Ding, A., 2018. Impact of aerosol-PBL interaction on haze pollution: multiyear observational evidences in North China. Geophys. Res. Lett. 45 (16), 8596–8603. https://doi.org/10.1029/2018gl079239.
Huang, X., Ding, A., Gao, J., Zheng, B., Zhou, D., Qi, X., He, K., 2020. Enhanced secondary pollution offset reduction of primary emissions during COVID-19 lockdown in China. Natl. Sci. Rev. 8 (2), nwaa137 https://doi.org/10.1093/nsr/nwaa137.
Huang, Q., Chu, Y., Li, Q., 2021. Climatology of low-level temperature inversions over China based on high-resolution radiosonde measurements. Theor. Appl. Climatol. 144 (1–2), 415–429. https://doi.org/10.1007/s00704-021-03536-w.
Iacono, M.J., Delamere, J.S., Mlawer, E.J., Shephard, M.W., Clough, S.A., Collins, W.D., 2008. Radiative forcing by long-lived greenhouse gases: calculations with the AER radiative transfer models. J. Geophys. Res. Atmos. 113 (D13), D13103 https://doi.org/10.1029/2008jd009944.
Jiang, C., Wang, H., Zhao, T., Li, T., Che, H., 2015. Modeling study of PM_{2.5} pollutant transport across cities in China's Jing–Jin–Ji region during a severe haze episode in December 2013. Atmos. Chem. Phys. 15 (10), 5803–5814. https://doi.org/10.5194/acp-15-5803-2015.
Jonsson, P., Bennet, C., Eliasson, I., Selin Lindgren, E., 2004. Suspended particulate matter and its relations to the urban climate in Dar es Salaam, Tanzania. Atmos. Environ. 38 (25), 4175–4181. https://doi.org/10.1016/j.atmosenv.2004.04.021.
Kalnay, E., Cai, M., 2003. Impact of urbanization and land-use change on climate. Nature 423 (6939), 528–531. https://doi.org/10.1038/nature01649.
Kim, D.-H., 2005. Aerosol radiative forcing over East Asia determined from ground-based solar radiation measurements. J. Geophys. Res. Atmos. 110 (D10), D10S22 https://doi.org/10.1029/2004jd004678.
Kusaka, H., Kimura, F., 2004. Coupling a single-layer urban canopy model with a simple atmospheric model: impact on urban Heat Island simulation for an idealized case. J. Meteorol. Soc. Japan. Ser. II 82 (1), 67–80. https://doi.org/10.2151/jmsj.82.67.
Li, M., Song, Y., Mao, Z., Liu, M., Huang, X., 2016. Impacts of thermal circulations induced by urbanization on ozone formation in the Pearl River Delta region, China. Atmos. Environ. 127, 382–392. https://doi.org/10.1016/j.atmosenv.2015.10.075.
Li, Z., Guo, J., Ding, A., Liao, H., Liu, J., Sun, Y., Zhu, B., 2017a. Aerosol and boundary-layer interactions and impact on air quality. Natl. Sci. Rev. 4 (6), 810–833. https://doi.org/10.1093/nsr/nwx117.
Li, M., Zhang, Q., Kurokawa, J.-I., Woo, J.-H., He, K., Lu, Z., Zheng, B., 2017b. MIX: a mosaic Asian anthropogenic emission inventory under the international collaboration framework of the MICS-Asia and HTAP. Atmos. Chem. Phys. 17 (2), 935–963. https://doi.org/10.5194/acp-17-935-2017.
Lin, Y.-L., Farley, R.D., Orville, H.D., 1983. Bulk parameterization of the snow field in a cloud model. J. Clim. Appl. Meteorol. 22 (6), 1065–1092. https://doi.org/10.1175/1520-0450(1983)022<1065:bpotsf>2.0.co;2.
Liu, X.G., Li, J., Qu, Y., Han, T., Hou, L., Gu, J., Hu, M., 2013. Formation and evolution mechanism of regional haze: a case study in the megacity Beijing, China. Atmos. Chem. Phys. 13 (9), 4501–4514. https://doi.org/10.5194/acp-13-4501-2013.
Liu, P., Song, H., Wang, T., Wang, F., Li, X., Miao, C., Zhao, H., 2020. Effects of meteorological conditions and anthropogenic precursors on ground-level ozone concentrations in Chinese cities. Environ. Pollut. 262, 114366 https://doi.org/10.1016/j.envpol.2020.114366.
Lo, J.C.F., Lau, A.K.H., Chen, F., Fung, J.C.H., Leung, K.K.M., 2007. Urban modification in a mesoscale model and the effects on the local circulation in the Pearl River Delta region. J. Appl. Meteorol. Climatol. 46 (4), 457–476. https://doi.org/10.1175/jam2477.1.
Manoli, G., Fatichi, S., Schläpfer, M., Yu, K., Crowther, T.W., Meili, N., Bou-Zeid, E., 2019. Magnitude of urban heat islands largely explained by climate and population. Nature 573 (7772), 55–60. https://doi.org/10.1038/s41586-019-1512-9.
Masson-Delmotte, V.P.Z.A., Pirani, S.L.C., Péan, C., Berger, S., Caud, N., Zhou, B., 2021. IPCC, 2021: Climate Change 2021: The Physical Science Basis. Contribution of Working Group I to the Sixth Assessment Report of the Intergovernmental Panel on Climate Change.
Meehl, G.A., Arblaster, J.M., Collins, W.D., 2008. Effects of black carbon aerosols on the Indian monsoon. J. Clim. 21 (12), 2869–2882. https://doi.org/10.1175/2007jcli1777.1.
Memon, R.A., Leung, D.Y., Chunho, L., 2008. A review on the generation, determination and mitigation of urban heat island. J. Environ. Sci. (China) 20 (1), 120–128. https://doi.org/10.1016/s1001-0742(08)60019-4.
Miao, S., Chen, F., LeMone, M.A., Tewari, M., Li, Q., Wang, Y., 2009. An observational and modeling study of characteristics of urban Heat Island and boundary layer structures in Beijing. J. Appl. Meteorol. Climatol. 48 (3), 484–501. https://doi.org/10.1175/2008jamc1909.1.
Miao, Y., Liu, S., Zheng, Y., Wang, S., Chen, B., 2015. Numerical study of the effects of topography and urbanization on the local atmospheric circulations over the Beijing-Tianjin-Hebei, China. Adv. Meteorol. 2015, 1–16. https://doi.org/10.1155/2015/397070.
Oke, T.R., 1973. City size and the urban heat island. Atmos. Environ. 7 (8), 769–779. https://doi.org/10.1016/0004-6981(73)90140-6.
Oke, T.R., 1982. The energetic basis of the urban heat island. Q. J. R. Meteorol. Soc. 108 (455), 1–24. https://doi.org/10.1002/qj.49710845502.
Otero, N., Sillmann, J., Schnell, J.L., Rust, H.W., Butler, T., 2016. Synoptic and meteorological drivers of extreme ozone concentrations over Europe. Environ. Res. Lett. 11 (2) https://doi.org/10.1088/1748-9326/11/2/024005.
Ramanathan, V., Crutzen, P.J., Kiehl, J.T., Rosenfeld, D., 2001. Aerosols, climate, and the hydrological cycle. Science 294 (5549), 2119–2124. https://doi.org/10.1126/science.1064034.
Ren, G.Y., Chu, Z.Y., Chen, Z.H., Ren, Y.Y., 2007. Implications of temporal change in urban heat island intensity observed at Beijing and Wuhan stations. Geophys. Res. Lett. 34 (5) https://doi.org/10.1029/2006gl027927.
Rosenfeld, D., 2008. Flood or drought: how do aerosols affect precipitation? Science 321, 1309.
Sarrat, C., Lemonsu, A., Masson, V., Guedalia, D., 2006. Impact of urban heat island on regional atmospheric pollution. Atmos. Environ. 40 (10), 1743–1758. https://doi.org/10.1016/j.atmosenv.2005.11.037.
Slater, J., Tonttila, J., McFiggans, G., Coe, H., Romakkaniemi, S., Xu, W., Fu, P., 2020. Using a coupled LES aerosol-radiation model to investigate the importance of aerosol-boundary layer feedback on a Beijing haze episode. Faraday Discuss. https://doi.org/10.1039/d0fd00085j.
Su, T., Li, Z., Zheng, Y., Wu, T., Wu, H., Guo, J., 2022. Aerosol-boundary layer interaction modulated entrainment process. Npj Clim Atmos Sci 5 (1). https://doi.org/10.1038/s41612-022-00283-1.
Sun, Y., Jiang, Q., Wang, Z., Fu, P., Li, J., Yang, T., Yin, Y., 2014. Investigation of the sources and evolution processes of severe haze pollution in Beijing in January 2013. J. Geophys. Res. Atmos. 119 (7), 4380–4398. https://doi.org/10.1002/2014jd021641.

Tao, W., Liu, J., Ban-Weiss, G.A., Hauglustaine, D.A., Zhang, L., Zhang, Q., Tao, S., 2015. Effects of urban land expansion on the regional meteorology and air quality of eastern China. Atmos. Chem. Phys. 15 (15), 8597–8614. https://doi.org/10.5194/acp-15-8597-2015.

Tewari, M., Chen, F., Kusaka, H., Miao, S., 2007. Coupled WRF/Unified Noah/Urban-Canopy Modeling System.

Wang, J., Wang, S., Jiang, J., Ding, A., Zheng, M., Zhao, B., Hao, J., 2014. Impact of aerosol–meteorology interactions on fine particle pollution during China's severe haze episode in January 2013. Environ. Res. Lett. 9 (9), 094002 https://doi.org/10.1088/1748-9326/9/9/094002.

Wang, Z., Huang, X., Ding, A., 2018. Dome effect of black carbon and its key influencing factors: a one-dimensional modelling study. Atmos. Chem. Phys. 18 (4), 2821–2834. https://doi.org/10.5194/acp-18-2821-2018.

Yang, X., Hou, Y., Chen, B., 2011. Observed surface warming induced by urbanization in East China. J. Geophys. Res. 116 (D14) https://doi.org/10.1029/2010jd015452.

Yang, P., Ren, G., Liu, W., 2013. Spatial and temporal characteristics of Beijing urban Heat Island intensity. J. Appl. Meteorol. Climatol. 52 (8), 1803–1816. https://doi.org/10.1175/jamc-d-12-0125.1.

Yang, G., Ren, G., Zhang, P., Xue, X., Tysa, S.K., Jia, W., Zhang, S., 2021. PM2.5 influence on urban Heat Island (UHI) effect in Beijing and the possible mechanisms. J. Geophys. Res. Atmos. 126 (17) https://doi.org/10.1029/2021jd035227.

Yu, H., Liu, S.C., Dickinson, R.E., 2002. Radiative effects of aerosols on the evolution of the atmospheric boundary layer. J. Geophys. Res. Atmos. 107 (D12) https://doi.org/10.1029/2001jd000754. AAC 3-1-AAC 3-14.

Yu, M., Carmichael, G.R., Zhu, T., Cheng, Y., 2014. Sensitivity of predicted pollutant levels to anthropogenic heat emissions in Beijing. Atmos. Environ. 89, 169–178. https://doi.org/10.1016/j.atmosenv.2014.01.034.

Zaveri, R.A., Peters, L.K., 1999. A new lumped structure photochemical mechanism for large-scale applications. J. Geophys. Res. Atmos. 104 (D23), 30387–30415. https://doi.org/10.1029/1999jd900876.

Zaveri, R.A., Easter, R.C., Fast, J.D., Peters, L.K., 2008. Model for simulating aerosol interactions and chemistry (MOSAIC). J. Geophys. Res. Atmos. 113 (D13), D13204 https://doi.org/10.1029/2007jd008782.

Zhang, N., Gao, Z., Wang, X., Chen, Y., 2010. Modeling the impact of urbanization on the local and regional climate in Yangtze River Delta, China. Theor. Appl. Climatol. 102 (3–4), 331–342. https://doi.org/10.1007/s00704-010-0263-1.

Zhang, X., Zhang, Q., Hong, C., Zheng, Y., Geng, G., Tong, D., Zhang, X., 2018. Enhancement of PM2.5 concentrations by aerosol-meteorology interactions over China. J. Geophys. Res. Atmos. 123 (2), 1179–1194. https://doi.org/10.1002/2017jd027524.

Zheng, G.J., Duan, F.K., Su, H., Ma, Y.L., Cheng, Y., Zheng, B., He, K.B., 2015. Exploring the severe winter haze in Beijing: the impact of synoptic weather, regional transport and heterogeneous reactions. Atmos. Chem. Phys. 15 (6), 2969–2983. https://doi.org/10.5194/acp-15-2969-2015.

Zhong, S., Qian, Y., Zhao, C., Leung, L., Yang, X.-Q., 2015. A case study of urbanization impact on summer precipitation in the greater Beijing metropolitan area: urban Heat Island versus aerosol effects. J. Geophys. Res. Atmos. 120, 10,903–10,914. https://doi.org/10.1002/2015JD023753.

Zhou, L., Dickinson, R.E., Tian, Y., Fang, J., Li, Q., Kaufmann, R.K., Myneni, R.B., 2004. Evidence for a significant urbanization effect on climate in China. Proc. Natl. Acad. Sci. 101 (26), 9540–9544. https://doi.org/10.1073/pnas.0400357101.

Zhou, D., Zhang, L., Hao, L., Sun, G., Liu, Y., Zhu, C., 2016. Spatiotemporal trends of urban heat island effect along the urban development intensity gradient in China. Sci. Total Environ. 544, 617–626. https://doi.org/10.1016/j.scitotenv.2015.11.168.